

ARTICLE OPEN

Interfacial orbital preferential occupation induced controllable uniaxial magnetic anisotropy observed in Ni/NiO(110) heterostructures

Yu-Jun Zhang¹, Liang Wu¹, Ji Ma¹, Qing-Hua Zhang¹, Atsushi Fujimori², Jing Ma¹, Yuan-Hua Lin¹, Ce-Wen Nan¹ and Nian-Xiang Sun³

Unexpected physical phenomena could emerge at heterostructure interfaces, and interface effects are also capable of giving rise to magnetic anisotropy. In this work, a peculiar uniaxial magnetic anisotropy in (polycrystalline Ni)/(epitaxial NiO)/SrTiO₃(110) heterostructures is investigated. Thickness dependence of the anisotropy confirms its interfacial effect nature. The NiO antiferromagnetic ordering induced interface exchange coupling should not be responsible for the anisotropy according to the temperature dependence. Our soft X-ray linear dichroism and magnetic circular dichroism results show a preferential occupation of orbital parallel to in-plane [100] at Ni/NiO interface and the origin of this uniaxial anisotropy is closely related to the occupation of Ni 3d orbitals at the interface. The magnetocrystalline anisotropy and piezoelectric strain could be utilized to manipulate this uniaxial anisotropy and realize controllable in-plane easy axis switching, which could be promising in future application of spintronics devices.

npj Quantum Materials (2017)2:17; doi:10.1038/s41535-017-0020-0

INTRODUCTION

Involving four performers named charge, spin, lattice, and orbital, heterostructure interfaces provide a charming stage for them to interact. Components with different charge distribution, spin ordering, lattice structure, and orbital occupation could couple with each other through the interfaces by charge transfer, spin reorientation, lattice epitaxial strain, and orbital reconstruction, leading to various novel physical phenomena and broadening the horizon of modern condensed matter physics.^{1–4} Not only contributing to the coupling between pre-existing properties of each components like antiferromagnet (AFM)/ferromagnet (FM) interface exchange coupling,^{5–7} magnetoelectric effects in multiferroic heterostructures,^{8–11} and oxygen octahedral coupling between perovskites,^{12–14} interface effects could also give rise to properties that each of the adjacent components does not possess, such as high-mobility two-dimensional electron gas^{15–17} at the interface of two insulators, which could also exhibit superconductivity^{18, 19} and magnetism.^{2, 20, 21} Interface engineering has already become a tantalizing subject, by working on which we can obtain abundant knowledge of basic physics concealed in heterostructure interfaces and develop new ideas for designing devices based on interface effects, which are applicable in future spintronics.

Interface effect induced magnetic anisotropy has also been a permanently attractive topic for researchers. Interface spin exchange interaction^{5, 6, 22–24} has become the first considered mechanism for interface magnetic anisotropy, which links the anisotropy of adjacent magnetically ordered components. For example, in exchange biased AFM/FM systems, magnetic anisotropy of ferromagnetic layer is controlled by anisotropy of AFMs through interface exchange coupling. Interfacial charge effect²⁵

has been proposed as an origin of magnetic anisotropy in (Ga,Mn)As diluted magnetic semiconductor systems, in which the magnetic anisotropy is linked to the carrier concentration. Strain effect^{12, 26–28} has also been put forward to explain various magnetic anisotropies in epitaxial thin films, which are under the constraint of substrate lattice. Epitaxial growth of thin films could provide not only strain-induced anisotropy, which will be relaxed several tens of nanometers away from the interface,²⁹ but also magnetocrystalline anisotropy, which will persist when the film thickness increases. Besides well-investigated exchange bias effect and strain-induced anisotropic magnetism, recently some new interfacial magnetic coupling mechanisms have been proposed in perovskite heterostructures. Z. Liao *et al.*¹² reported an interfacial octahedral coupling caused magnetic anisotropy in manganese epitaxial films and D. Kan *et al.*³⁰ observed that oxygen coordination environment could dominate the magnetic anisotropy in a SrRuO₃/Ca_{0.5}Sr_{0.5}TiO₃/GaScO₃(110) heterostructure. Lattice modulation of magnetic anisotropy could be realized by not only tuning the lattice constants and tetragonality.

As mentioned above, interactions of spin, charge, and lattice at the interfaces could contribute to emergent magnetic anisotropy. Orbital could be another way to induce and control magnetic anisotropy. Metal multilayers like Co/Pt^{31, 32} and Co/Pd^{33, 34} could exhibit perpendicular magnetic anisotropy, which was reported to originate from preferential out-of-plane interfacial orbital occupation.³² Nevertheless, in-plane magnetic anisotropy dominated by interfacial spin-orbit interaction has not yet been investigated up to now. In this work, we demonstrate a polycrystalline ferromagnetic nickel layer grown on NiO(110) epitaxial film exhibiting an in-plane easy axis. The thickness and temperature dependences have been investigated in details. The synchrotron X-ray linear

¹State Key Lab of New Ceramics and Fine Processing, School of Materials Science and Engineering, Tsinghua University, Beijing 100084, China; ²Department of Physics, University of Tokyo, 7-3-1 Hongo, Bunkyo-ku, Tokyo 113-0033, Japan and ³Electric and Computer Engineering Department, Northeastern University, Boston, MA 02115, USA
Correspondence: Yuan-Hua Lin (linyh@tsinghua.edu.cn)

Received: 26 October 2016 Revised: 12 February 2017 Accepted: 23 February 2017

Published online: 20 March 2017

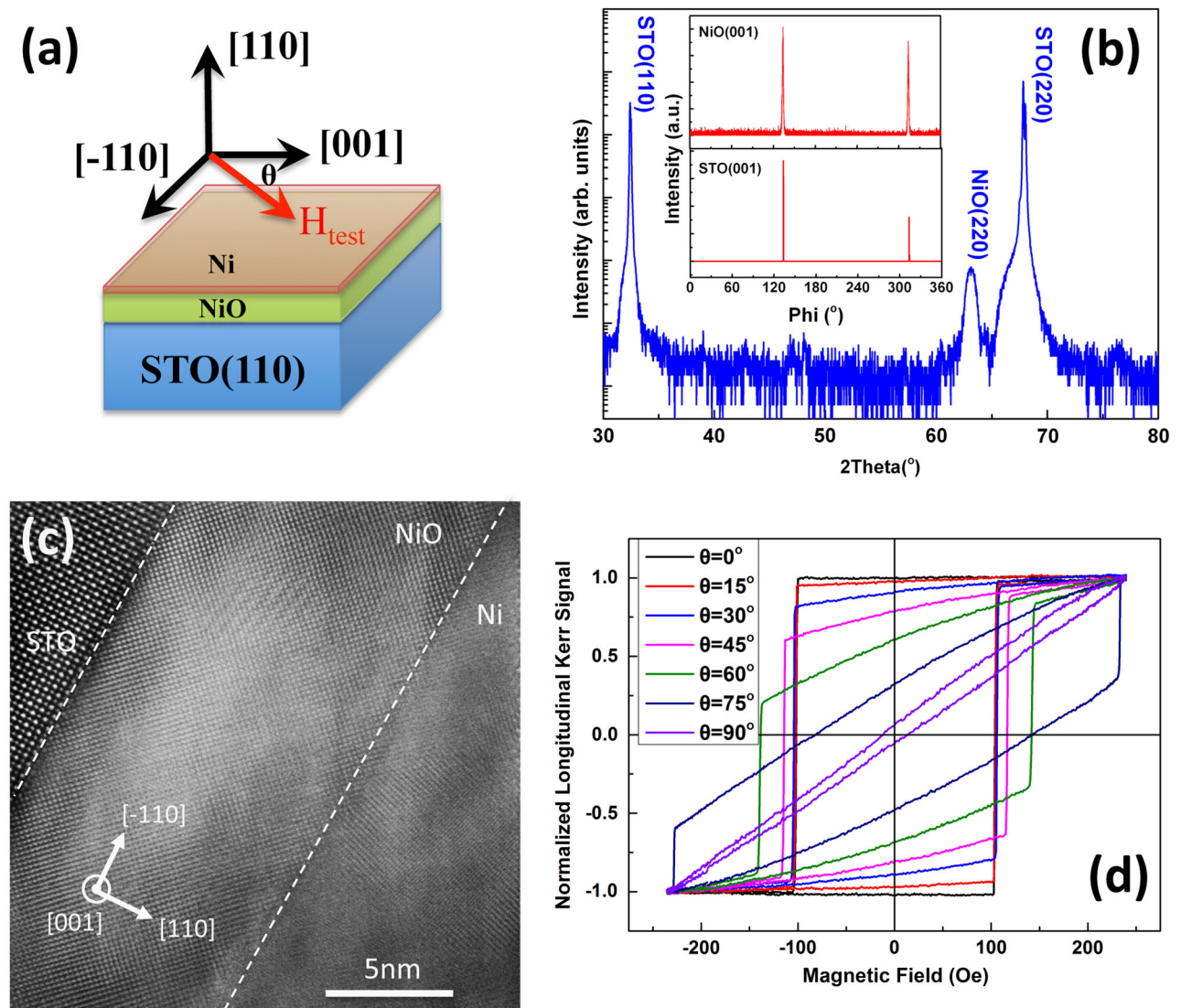


Fig. 1 Uniaxial anisotropy observed in Ni/NiO/SrTiO₃(110) heterostructure. **a** Schematics of Ni/NiO/SrTiO₃(110) heterostructure and the angle between measurement field and in-plane [001] direction is defined as θ . **b** Typical θ - 2θ X-ray diffraction spectrum of Ni(20 nm)/NiO(24 nm)/SrTiO₃(110) heterostructure. Inset shows the φ -scan spectra of both NiO{100} and SrTiO₃{100} groups of crystal planes, which indicates good in-plane epitaxy quality of NiO film. **c** Annular bright-field STEM images of Ni(20 nm)/NiO(24 nm)/SrTiO₃(110) heterostructure. **d** Magneto-optical Kerr effect measured anisotropic M-H loops of Ni(20 nm)/NiO(24 nm)/SrTiO₃(110) heterostructure, θ varied from 0° to 90°

dichroism (XLD) and X-ray magnetic circular dichroism (XMCD) spectra confirm the anisotropic Ni 3d orbital occupancy of NiO at the Ni/NiO interface as the origin of this peculiar magnetic anisotropy. Several ways to manipulate this in-plane anisotropy are also mentioned afterwards.

RESULTS

Figure 1 displays a first sight of the main results. Figure 1a is a schematic of the sample structure. The angle between the measuring magnetic field and the in-plane [001] direction is defined as θ . The NiO layer shows epitaxial growth on the SrTiO₃(110) substrate and the Ni layer exhibits a polycrystalline nature without visible texture, which is confirmed by X-ray diffraction patterns (Fig. 1b) and scanning transmission electron microscopy (STEM) cross-section images of the heterostructures (Fig. 1c). At room temperature, for typical Ni/NiO/SrTiO₃(110) heterostructure, Ni layer shows an emergent strong in-plane anisotropy (Fig. 1d) with easy axis lying parallel to [001] direction ($\theta = 0^\circ$). SQUID (superconducting quantum interference device,

quantum design) measured results presented in Supplementary Fig. 1 indicate a hard axis in out-of-plane direction and isotropic saturated magnetization in different directions.

To probe into the interface coupling origin of this uniaxial anisotropy, we investigated the film thickness dependence and varied the thickness of NiO from 0 to 24 nm and the thickness of Ni layer from 10 to 60 nm. Figure 2 shows the thickness dependence of the easy axis coercive field ($H_{c[001]}$) and the M_r ratio (defined as $M_{r[-110]}/M_{r[001]}$, where $M_{r[-110]}$ and $M_{r[001]}$ are the normalized residual magnetizations in [-110] and [001], respectively). The M_r ratio can represent the qualitative strength of the uniaxial anisotropy. $M_{r[-110]}/M_{r[001]} = 0$ indicates the strong uniaxial anisotropy and $M_{r[-110]}/M_{r[001]} = 1$ indicates no uniaxial anisotropy. The mentioned uniaxial anisotropy could also induce an obvious enhancement of $H_{c[001]}$. Fixing Ni thickness at 10 nm, when NiO thickness increases over a critical value of 3.2 nm, the uniaxial anisotropy could be established with the greatly enhanced easy axis coercive field, indicating the crucial role of NiO layer in modulating this anisotropy. The critical thickness value is closely related to the substrate, whose lattice mismatch with NiO could

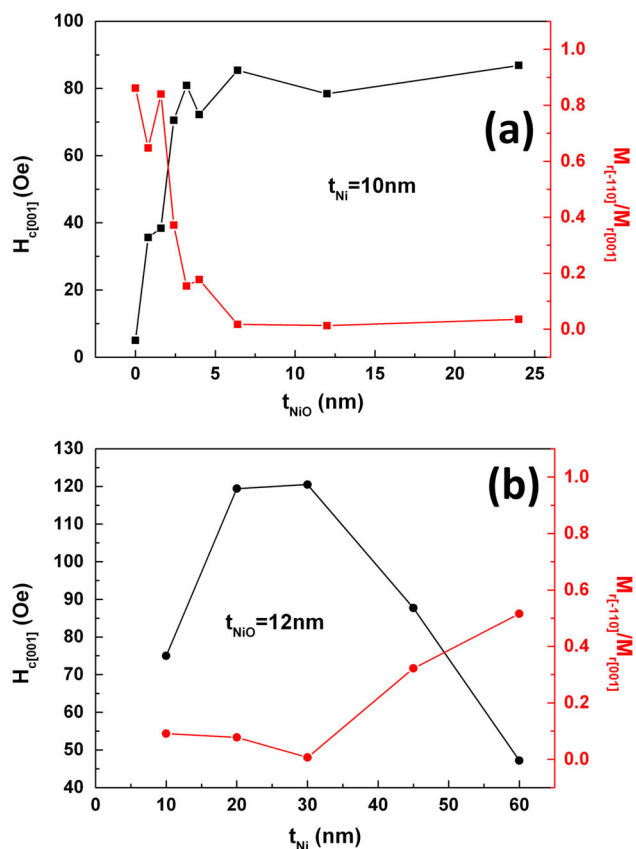


Fig. 2 Thickness dependence of the uniaxial anisotropy. **a** NiO layer thickness dependences of the easy axis coercive field $H_{c[001]}$ and the M_r ratio in the Ni(10 nm)/NiO/SrTiO₃(110) heterostructure. **b** Ni layer thickness dependences of easy axis coercive field and M_r ratio in the Ni/NiO(12 nm)/SrTiO₃(110) heterostructure

lead to different epitaxy qualities of the thin NiO layers, with the details illustrated in Supplementary Note 2. Take MgO(110) substrate as an instance, whose lattice parameter is very close to NiO. The critical thickness can be lowered to 0.8 nm (Supplementary Fig. 2a). However, on SrTiO₃(110) substrate, ultrathin NiO films will show some mismatch induced worse epitaxy quality, which will induce the weakening of magnetic anisotropy (Supplementary Fig. 2b). Fixing NiO layer thickness at 12 nm, the strong uniaxial anisotropy and easy axis coercive field enhancement could be maintained up to Ni layer thickness of 30 nm. When Ni layer is over 45 nm in thickness, the uniaxial anisotropy is weakened and the coercive field tends to the value for Ni single layer without NiO. Since the easy axis coercive field is determined by both uniaxial anisotropy and Ni thickness, the lower H_c of Ni(10 nm)/NiO(12 nm) sample than Ni(20 nm)/NiO(12 nm) sample, shown in Fig. 2b, could be attributed to the finite thickness effect. This Ni thickness dependence supports that the anisotropy originates from interface effect. As displayed in Supplementary Fig. 3, NiO layer roughness dependence also sheds light upon the interface effect nature of this anisotropy. This uniaxial anisotropy could be weakened or even destroyed unless the NiO epitaxial layer has low surface roughness. From these results, it could be inferred that the Ni/NiO interface effect plays a dominating role in the uniaxial anisotropy and the effect of magnetocrystalline anisotropy in the Ni layer is insignificant. Furthermore, possible substrate strain effect applied to NiO layer should also be ruled out because replacing SrTiO₃(110) (lattice constant 0.3905 nm) substrate by MgO(110) (lattice constant 0.421 nm) or Pb(Mg_{1/3}Nb_{2/3})O₃-PbTiO₃(110) (PMN-PT, 30% PbTiO₃, lattice constant 0.4022 nm) substrate, which could impose tensile

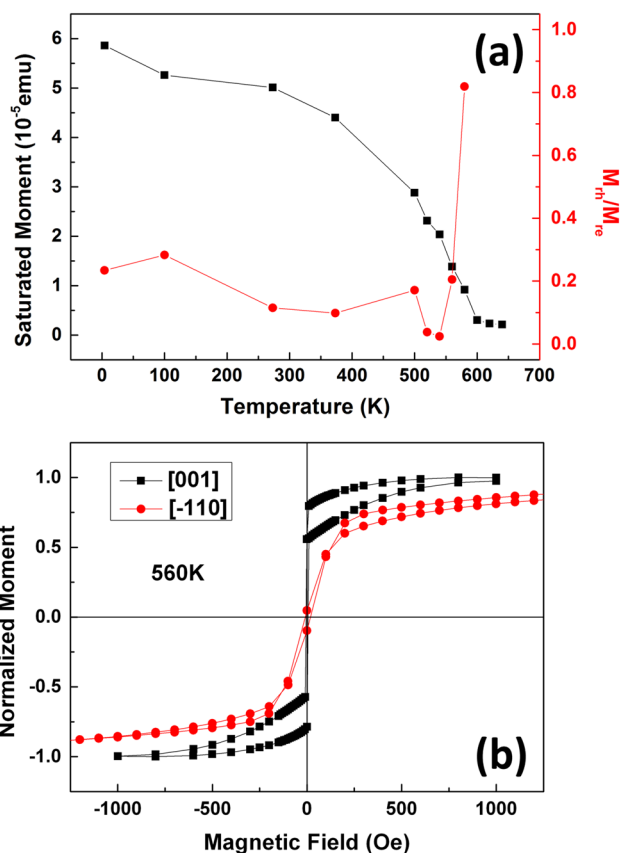


Fig. 3 Temperature dependence of the uniaxial anisotropy. **a** Temperature dependences of the magnetic moment and M_r ratio of Ni(20 nm)/NiO(12 nm)/SrTiO₃(110) heterostructure. **b** Easy and hard axis M-H curves of Ni(20 nm)/NiO(12 nm)/SrTiO₃(110) heterostructure measured at 560 K

or compressive epitaxial strain to the NiO layer, cannot change the uniaxial anisotropy significantly (Supplementary Fig. 4).

As NiO is a typical antiferromagnetic material, if the magnetic moments of (110) oriented NiO film could exhibit some kind of in-plane magnetic anisotropy, the interfacial AFM/FM exchange coupling could be an origin of this uniaxial anisotropy. However, the temperature dependence of the uniaxial anisotropy, as shown in Fig. 3, rules out the mechanism of AFM/FM magnetic coupling. The uniaxial anisotropy could exist up to 560 K for the Ni/NiO/SrTiO₃(110) heterostructure, which is higher than the bulk Neel temperature of NiO (525 K)³⁵. On the other hand, up to 1 T magnetic field-cooling from above the Neel temperature of NiO cannot induce visible exchange bias, as shown in Supplementary Fig. 5, indicating that the anisotropy does not have a typical AFM/FM coupling origin.

Ruling out the magnetocrystalline anisotropy in both Ni and NiO layers, epitaxial strain, and exchange coupling as origins of the uniaxial anisotropy, anisotropic interface orbital occupation could be another possible origin. If the Ni layer deposited on NiO (110) crystal plane could provide extra anisotropic 3d orbital occupancy at the interface, assuming that it exists above Neel temperature of NiO, the spin-orbit interaction may induce an easy axis to align the Ni ionic spins parallel to the preferentially occupied orbitals. Then the ferromagnetic layer could couple to these aligned interfacial spins and exhibit uniaxial anisotropy. To verify this idea, synchrotron XLD measurement was employed to detect the interface orbital preferential occupation. As schematically shown in Fig. 4a, with normal incidence to the films, two distinct soft X-ray absorption spectra (XAS) were measured with

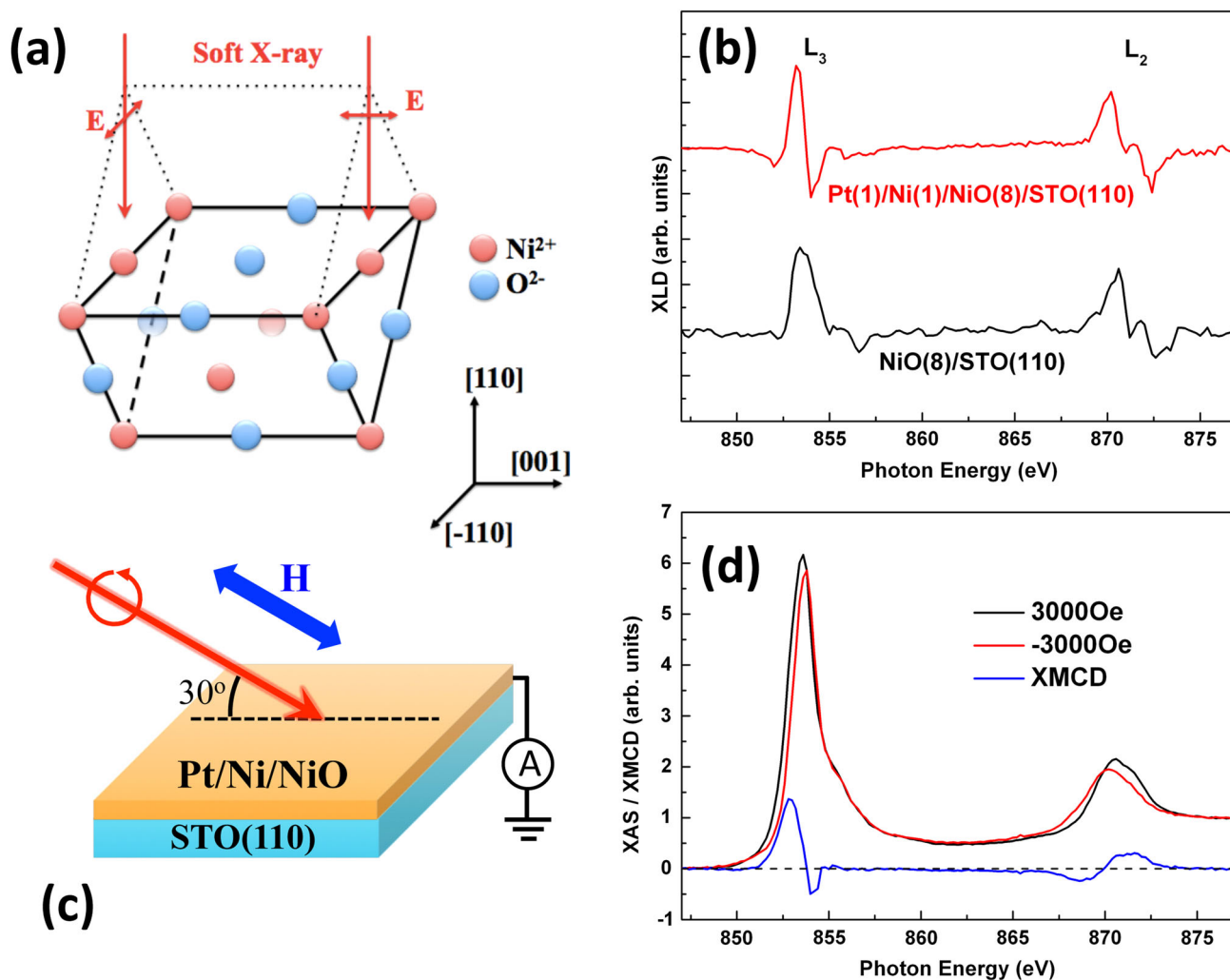


Fig. 4 Orbital preferential occupation of NiO 3d orbital in Ni/NiO/SrTiO₃(110) heterostructures. **a** The schematic of the XLD measurement shows that X-ray is perpendicularly incident and possesses different electric field vectors parallel to [001] or [-110] directions of the substrate. Absorption of different linearly polarized X-ray corresponds to the number of empty states in orbitals parallel to [001] and [-110]. **b** XLD spectra of NiO(8 nm)/SrTiO₃(110) and Pt(1 nm)/Ni(1 nm)/NiO(8 nm)/SrTiO₃(110) heterostructures. **c** Schematic of the XMCD measurement. **d** Circularly polarized XAS and XMCD spectra of Pt(1 nm)/Ni(1 nm)/NiO(8 nm)/SrTiO₃(110) sample with applied ± 3000 Oe magnetic field

the X-ray electric field vector E parallel to [001] and [-110], respectively. The overall linearly polarized XAS spectra are displayed in Supplementary Fig. 6. The XLD intensity is defined as the intensity difference between the absorption of $E//[001]$ and $E//[-110]$ linearly polarized X-rays, namely, $XLD = XAS(E//[001]) - XAS(E//[-110])$. As Ni L-edge XAS spectra reflect the atomic $2p^6 3d^8 - 2p^5 3d^9$ transition in the samples, positive XLD intensity represents holes in the d orbital parallel to [001] and negative XLD intensity represents holes in the d orbital parallel to [-110]³⁶. Considering the detection depth of the total electron yield (TEY) mode in the XLD measurement³⁷, thinner metal layers are necessary for detecting the signal of NiO layer at the interface, as detailedly discussed in Supplementary Note 6. Although in our sample, the 1 nm Ni layer is not thick enough for us to detect the magnetic anisotropy directly due to its weak magnetization, it would be sufficient to extract information about the chemical bonding and the orbital reconstruction at the interface. The XLD spectra of the NiO(8 nm)/SrTiO₃(110) and Pt(1 nm)/Ni(1 nm)/NiO(8 nm)/SrTiO₃(110) heterostructures are displayed in Fig. 4b. The XLD signal of NiO/SrTiO₃(110) structure could reflect the preferential orbital occupancy of the (110)-oriented NiO thin film, which could be induced by the nonrelaxed substrate strain or possible texture of Ni ionic magnetic moments. As compared to the XLD signal of

NiO/SrTiO₃(110), Ni/NiO/SrTiO₃(110) heterostructures exhibit obvious difference of XLD line shape at the L₃ edge. Considering the polycrystalline nature of Ni layer and the much smaller contribution of magnetic XLD signal in 3d ferromagnetic metals³⁸, the contribution of 1 nm Ni metal layer could be reasonably neglected. Therefore, the difference of XLD signal between NiO/SrTiO₃(110) and Ni/NiO/SrTiO₃(110) indicates preferential occupation of 3d orbital parallel to [001] at the Ni/NiO interface compared to the bare (110) oriented NiO. It can be seen that the L₃ XLD spectrum of NiO/SrTiO₃(110) structure only shows a positive peak, and that of Ni/NiO/SrTiO₃(110) structure shows two overlapped positive and negative peaks, which indicates a combination of occupation in both orbitals parallel to [001] and [-110]. Therefore, the Ni metal deposition can induce preferential occupation in the orbitals parallel to [001]. As for the L₂ edge, the difference between NiO/SrTiO₃(110) and Ni/NiO/SrTiO₃(110) is not significant, but there is still similar character as the L₃ edge, which is probably because the Ni $2p_{1/2}$ core-level (L₂ edge) wave function is more isotropic than the Ni $2p_{3/2}$ (L₃ edge). To explore the evidence that the uniaxial anisotropy in Ni layer is connected to the preferential occupation of Ni 3d orbitals in NiO, XMCD measurement was performed for the Ni/NiO/SrTiO₃ sample as well. The circularly polarized soft X-ray was utilized and ± 3000 Oe magnetic field was

applied along the X-ray propagation. The X-ray incident angle was set at 30° to achieve an in-plane component of the magnetic field. In Fig. 4d, not only XMCD signal of Ni layer at the photon energy of 852.8 and 868.6 eV but also XMCD signal of NiO layer at higher energy of 854.2 and 871.2 eV could be observed. And dramatically, the induced moment in NiO is coupled to the Ni moments with an antiparallel configuration according to the opposite sign of their XMCD signals. According to the sum-rule of XMCD spectra^{39, 40}, the non-identical integrated area of NiO moments at L₃ and L₂ edges indicates a finite magnetic moment with both orbital and spin components. These spectroscopic results are consistent with the conclusion that the observed easy axis along [001] (Fig. 1d) has the origin that the spin-orbit coupling and interface exchange interaction connect the preferential occupied Ni ionic orbitals with the magnetic moments in Ni metal.

DISCUSSION

Up to now, we have elucidated the mechanism of this peculiar interface effect induced in-plane anisotropy in the Ni/NiO/SrTiO₃(110) heterostructure. Consequently, we can propose two methods to tune this anisotropy, switching the easy-axis between the in-plane [001] and [-110] directions. The first method is varying the ferromagnetic layer composition from Ni to Co. As demonstrated in Fig. 5a, b, we observed a continuous shift of the easy axis in Ni_{1-x}Co_x/NiO/SrTiO₃(110) heterostructures. The Co film could exhibit easy axis in in-plane [-110] direction, which is likely to be induced by magnetocrystalline anisotropy. Only a small amount of Co doping in Ni layer will weaken the in-plane [001] easy axis anisotropy. For the nominal ferromagnetic layer composition of Ni₇₅Co₂₅, the easy axis was shifted to the in-plane [-110] direction. We also prepared the same ferromagnetic films without NiO layer on SrTiO₃(110) substrates and observed a transition from isotropic ferromagnetism to uniaxial anisotropy in [-110] direction at the same film composition where the easy axis shifts from [001] to [-110] in the Ni_{1-x}Co_x/NiO/SrTiO₃(110) heterostructures, which is shown in Fig. 5c. However, considering the possible influence of texture and magnetocrystalline anisotropy, which is described in Supplementary Note 7, we cannot clearly determine whether there is any contribution of above-mentioned interface effect induced anisotropy in the Ni_{1-x}Co_x/NiO/SrTiO₃(110) heterostructures.

Besides varying the film composition, another way to manipulate the uniaxial anisotropy in a certain heterostructure is to grow Ni/NiO bilayer on perovskite ferroelectric single crystal, like Pb(Mg_{1/3}Nb_{2/3})O₃-PbTiO₃(110) substrate. The basic idea is shown in Fig. 6a. In this heterostructure, NiO can maintain its epitaxial growth and the uniaxial anisotropy in the Ni layer will be preserved as illustrated above. A large enough out-of-plane electric field will saturate the ferroelectric substrate and induce a uniaxial compressive strain in the in-plane [-110] direction of the Ni film grown on it.^{41–43} Considering the negative magnetostriction coefficient of Ni film, a piezoelectricity induced easy axis along [-110] will emerge and compete with the original interface effect induced uniaxial anisotropy along [001]. Therefore, we can use electric field to switch the easy axis between the in-plane [001] and [-110] directions. Figure 6b, c demonstrate the electric field manipulation of the uniaxial anisotropy. In order to get a proper strength of anisotropy in [001] direction, the NiO layer thickness is chosen to be 1.6 nm to weaken the interface effect induced anisotropy. After a +0.8 MV/m electric field pre-poling, the anisotropy of Ni layer is dominated by the piezoelectricity induced uniaxial anisotropy, whose easy axis is lying in [-110]. When an out-of-plane electric field of -0.15 MV/m is applied, the ferroelectric domains switch to in-plane directions and the Ni/NiO interface induced anisotropy appears. Larger negative electric field will again switch the ferroelectric domains to out-of-plane directions and induce easy axis in [-110]. In our experiments,

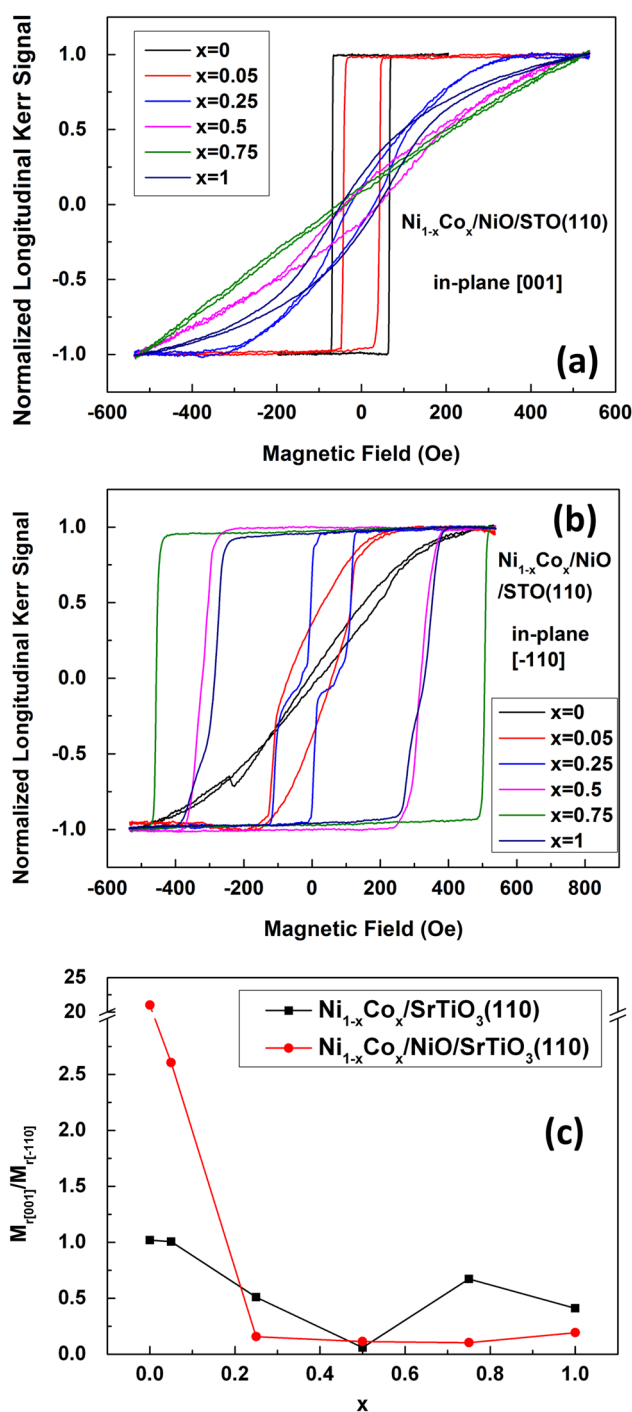


Fig. 5 Shifting of easy axis in Ni_{1-x}Co_x(10 nm)/NiO(12 nm)/SrTiO₃(110) heterostructure. MOKE measured M-H curves of different x in **a** [001] and **b** [-110] directions. **c** Composition dependence of M_r ratio in Ni_{1-x}Co_x(10 nm)/NiO(12 nm)/SrTiO₃(110) and Ni_{1-x}Co_x(10 nm)/SrTiO₃(110) heterostructures. Note that compared to the definition in Fig. 2, the M_r ratio is inverted for convenience of comprehension. With this definition the M_r ratio is varying from 0 (strong uniaxial anisotropy in [-110]) to 1 (weak uniaxial anisotropy in [-110]) in the x range of 0.25~1. When x=0 the uniaxial anisotropy is strong but shifted to [001] and the value of M_r ratio becomes much more than 1

the easy axis switching is reproducible and non-volatile after the removal of electric field. Note that this piezoelectric effect induced strain is different from the substrate strain mentioned before because the piezoelectric strain is applied to the whole Ni/NiO

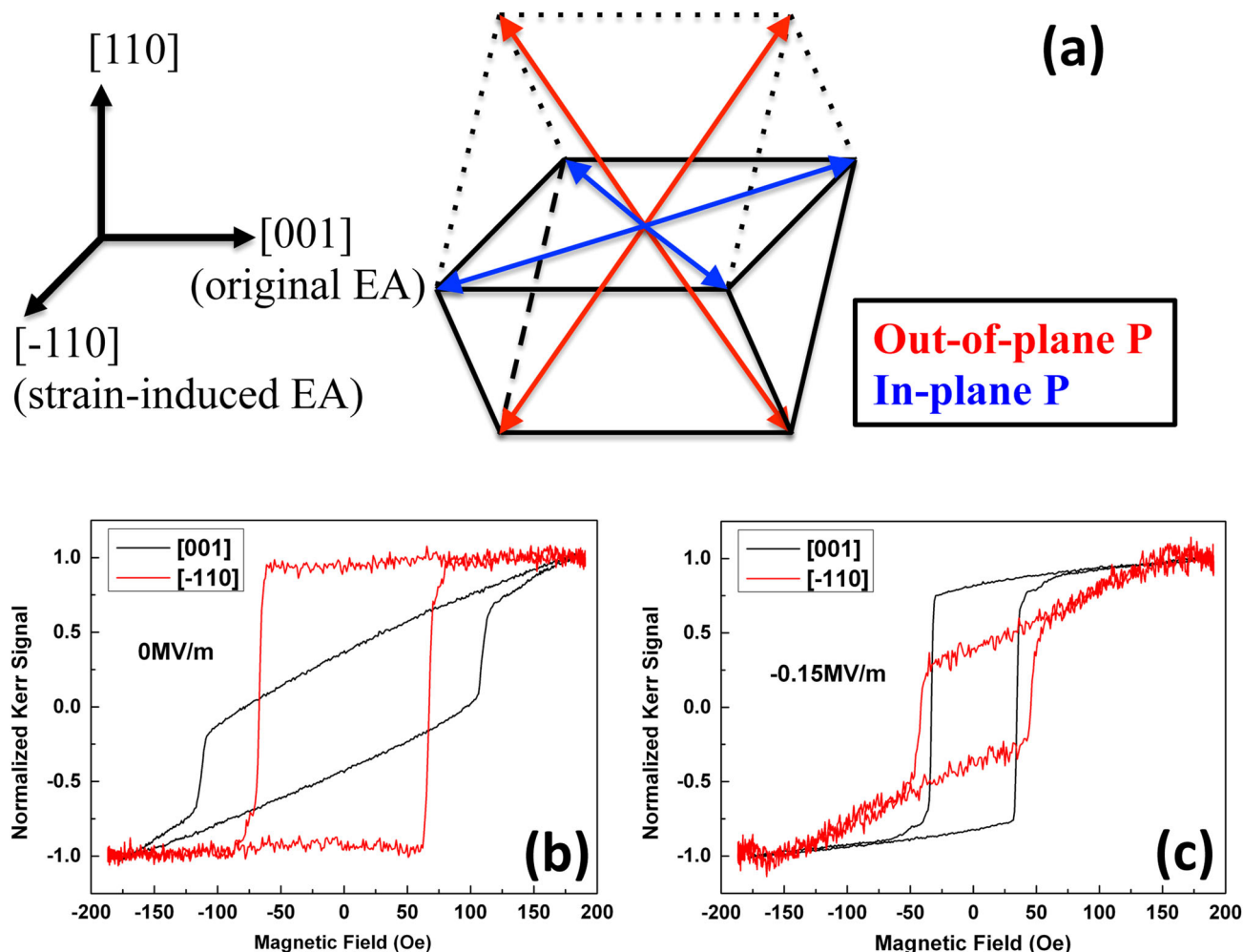


Fig. 6 Electric field manipulation of uniaxial anisotropy. **a** Schematic of the polarization directions of PMN-PT(110) ferroelectric single crystal substrates. Switching the polarization from in-plane to out-of-plane could induce an anisotropic compressive strain in $[-110]$, which will generate an easy axis of Ni layer in the same direction. **b**, **c** MOKE measured M-H loops of the Ni(10 nm)/NiO(1.6 nm)/PMN-PT(110) heterostructure with different out-of-plane electric fields. A $+0.8$ MV/m electric field is applied to pre-polarize the PMN-PT(110) substrate. To reflect the magnetic properties of the same area on the sample, M-H loops of $[001]$ and $[-110]$ directions are measured by longitudinal and transverse Kerr effect, respectively, which could be carried out simultaneously

bilayer but the substrate strain comes from the lattice mismatch between NiO and the substrate. The substrate strain could not be felt by the consequently deposited polycrystalline Ni layer and does not affect the magnetic anisotropy directly.

In conclusion, a peculiar uniaxial anisotropy is observed in Ni/NiO/SrTiO₃(110) heterostructures, which could be attributed to interfacial orbital reconstruction and spin-orbit coupling at the Ni/NiO interface. The easy realization of stable in-plane uniaxial anisotropy in polycrystalline magnetic thin films is of significance for magnetic heterostructure designing, where a uniaxial anisotropy is required. Two applicable methods are also presented to control the anisotropy axis in ferromagnetic layer/NiO heterostructure and may be quite useful for future spintronics devices, which expect to utilize the tunable in-plane uniaxial magnetic anisotropy.

METHODS

Thin film fabrication

The NiO layer was synthesized by a pulsed laser deposition method, using a KrF excimer pulsed laser ($\lambda = 248$ nm) with a repetition rate of 5 Hz and an energy density of 1.4 J/cm². The deposition temperature and ambient oxygen pressure were controlled at 650 °C and 50 mTorr, respectively, and

the distance between the NiO target and substrate was set at 8 cm, resulting a growth rate of 0.8 nm/min of the NiO thin films. After the NiO film deposition, the samples were transferred into a magnetron sputtering chamber with a background vacuum better than 3×10^{-7} Torr. DC sputtering was employed to grow the ferromagnetic metal layer and a Pt cap layer to prevent oxidation. Ferromagnetic layers were grown with a power of 40–45 W and a substrate temperature of 300 °C (growth rate 1.5 nm/min). For the Ni_{1-x}Co_x alloy films, according to the requested atomic ratio, fan-shaped Co target with central angle corresponding to the Co atomic percentage was placed on Ni target to achieve the nominal film compositions. After the ferromagnetic layer growth, the samples were cooled down in high vacuum and a 2 nm Pt cap layer was grown at room temperature with a DC power of 10 W. The substrate rotation was applied to avoid any sputtering incidence induced anisotropy. The as-deposited NiO films have a roughness of about 200 pm and after Ni deposition, the roughness of the samples is below 1 nm.

Characterization

The phase composition and the epitaxial relationship to the substrate of the thin films were characterized by a Rigaku (Tokyo, Japan) SMARTLAB X-ray diffractometer with Cu K α radiation. Microstructure characterization was carried out by a STEM (JEOL ARM200CF). SQUID and MOKE (magneto-optic Kerr effect, NanoMOKE2, quantum design) were employed to characterize the magnetic properties. The MOKE system utilizes a laser

of 633 nm wavelength and the spot size is around 5 μm . Room temperature soft XAS measurements were performed at the Beamline BL08U1A of Shanghai Synchrotron Radiation Facility, using the TEY mode. The normalization procedure of the XAS spectra is applied by dividing a factor and setting the L_3 pre-edge as 0 and the L_2 post-edge as 1.

ACKNOWLEDGEMENTS

This work was financially supported by the National Key Research Programme of China, under grant No. 2016YFA0201003, NSF of China (51272121, 51328203, 51332001, and 51532003), and a Grant-in-Aid for Scientific Research from JSPS (15H02109). We are also grateful to the discussion and support provided by staff in Beamline BL08U1A of Shanghai Synchrotron Radiation Facility.

AUTHOR CONTRIBUTIONS

Y.Z. prepared the samples. Y.Z. and L.W. measured the magnetic properties. Q.Z. did the STEM measurement. Y.Z. and Ji Ma collected and analyzed the XLD data with help from A.F., and Jing Ma, Y.L.C.N. and N.S. planned and supervised the study. Y.Z. wrote the manuscript with modification from A. F. and Y. L. All authors contributed to the discussion of the data.

COMPETING INTERESTS

The authors declare no competing interests.

REFERENCES

- Hwang, H. Y. et al. Emergent phenomena at oxide interfaces. *Nat. Mater.* **11**, 103–113 (2012).
- Yamada, H., Kawasaki, M., Lottermoser, T., Arima, T. & Tokura, Y. LaMnO₃/SrMnO₃ interfaces with coupled charge-spin-orbital modulation. *Appl. Phys. Lett.* **89**, 052506 (2006).
- Oka, T. & Nagaosa, N. Interfaces of correlated electron systems: proposed mechanism for colossal electroresistance. *Phys. Rev. Lett.* **95**, 266403 (2005).
- Chakhalian, J. et al. Orbital reconstruction and covalent bonding at an oxide interface. *Science* **318**, 1114–1117 (2007).
- Nogues, J. et al. Exchange bias in nanostructures. *Phys. Rep.* **422**, 65–117 (2005).
- Nogues, J. & Schuller, I. K. Exchange bias. *J. Magn. Magn. Mater.* **192**, 203–232 (1999).
- Liu, Z. et al. Epitaxial growth of intermetallic MnPt films on oxides and large exchange bias. *Adv. Mater.* **28**, 118–123 (2016).
- Kim, Y. M. et al. Direct observation of ferroelectric field effect and vacancy-controlled screening at the BiFeO₃/La₂Sr_{1-x}MnO₃ interface. *Nat. Mater.* **13**, 1019–1025 (2014).
- Kosub, T., Kopte, M., Radu, F., Schmidt, O. G. & Makarov, D. All-electric access to the magnetic-field-invariant magnetization of antiferromagnets. *Phys. Rev. Lett.* **115**, 097201 (2015).
- Weisheit, M. et al. Electric field-induced modification of magnetism in thin-film ferromagnets. *Science* **315**, 349–351 (2007).
- Chu, Y. H. et al. Electric-field control of local ferromagnetism using a magneto-electric multiferroic. *Nat. Mater.* **7**, 478–482 (2008).
- Liao, Z. et al. Controlled lateral anisotropy in correlated manganite heterostructures by interface-engineered oxygen octahedral coupling. *Nat. Mater.* **15**, 425–431 (2016).
- Borisevich, A. Y. et al. Suppression of octahedral tilts and associated changes in electronic properties at epitaxial oxide heterostructure interfaces. *Phys. Rev. Lett.* **105**, 087204 (2010).
- He, J., Borisevich, A., Kalinin, S. V., Pennycook, S. J. & Pantelides, S. T. Control of octahedral tilts and magnetic properties of perovskite oxide heterostructures by substrate symmetry. *Phys. Rev. Lett.* **105**, 227203 (2010).
- Ando, T., Fowler, A. B. & Stern, F. Electronic-properties of two-dimensional systems. *Rev. Mod. Phys.* **54**, 437–672 (1982).
- Ohtomo, A. & Hwang, H. Y. A high-mobility electron gas at the LaAlO₃/SrTiO₃ heterointerface. *Nature* **427**, 423–426 (2004).
- Caviglia, A. D. et al. Electric field control of the LaAlO₃/SrTiO₃ interface ground state. *Nature* **456**, 624–627 (2008).
- Reyren, N. et al. Superconducting interfaces between insulating oxides. *Science* **317**, 1196–1199 (2007).
- Ahn, C. H., Triscone, J. M. & Mannhart, J. Electric field effect in correlated oxide systems. *Nature* **424**, 1015–1018 (2003).

- Brinkman, A. et al. Magnetic effects at the interface between non-magnetic oxides. *Nat. Mater.* **6**, 493–496 (2007).
- Takahashi, K. S., Kawasaki, M. & Tokura, Y. Interface ferromagnetism in oxide superlattices of CaMnO₃/CaRuO₃. *Appl. Phys. Lett.* **79**, 1324–1326 (2001).
- Meiklejohn, W. H. Exchange anisotropy - a review. *J. Appl. Phys.* **33**, 1328–1335 (1962).
- Manna, P. K. & Yusuf, S. M. Two interface effects: exchange bias and magnetic proximity. *Phys. Rep.* **535**, 61–99 (2014).
- Malozemoff, A. P. Mechanisms of exchange-anisotropy. *J. Appl. Phys.* **63**, 3874–3879 (1988).
- Chiba, D. et al. Magnetization vector manipulation by electric fields. *Nature* **455**, 515–518 (2008).
- Boschker, H. et al. Strong uniaxial in-plane magnetic anisotropy of (001)- and (011)-oriented La_{0.67}Sr_{0.33}MnO₃ thin films on NdGaO₃ substrates. *Phys. Rev. B* **79**, 214425 (2009).
- Boeglin, C., Stanescu, S., Deville, J. P., Ohresser, P. & Brookes, N. B. In-plane magnetocrystalline anisotropy observed on Fe/Cu(111) nanostructures grown on stepped surfaces. *Phys. Rev. B* **66**, 014439 (2002).
- Dagotto, E. Complexity in strongly correlated electronic systems. *Science* **309**, 257–262 (2005).
- Vandermerwe, J. H. Crystal interfaces .2. Finite overgrowths. *J. Appl. Phys.* **34**, 123–127 (1963).
- Kan, D. et al. Tuning magnetic anisotropy by interfacially engineering the oxygen coordination environment in a transition metal oxide. *Nat. Mater.* **15**, 432–437 (2016).
- Lee, C. H., Farrow, R. F. C., Lin, C. J., Marinero, E. E. & Chien, C. J. Molecular-beam-epitaxial growth and magnetic-properties of Co-Pt superlattices oriented along the [001], [110], and [111] axes of Pt. *Phys. Rev. B* **42**, 11384–11387 (1990).
- Weller, D. et al. Orbital magnetic-moments of Co in multilayers with perpendicular magnetic-anisotropy. *Phys. Rev. B* **49**, 12888–12896 (1994).
- Lee, J. B. et al. Thermally robust perpendicular Co/Pd-based synthetic antiferromagnetic coupling enabled by a W capping or buffer layer. *Sci. Rep.* **6**, 21324 (2016).
- Carcia, P. F., Meinhardt, A. D. & Suna, A. Perpendicular magnetic-anisotropy in Pd/Co thin-film layered structures. *Appl. Phys. Lett.* **47**, 178–180 (1985).
- Roth, W. L. & Slack, G. A. Antiferromagnetic structure and domains in single crystal NiO. *J. Appl. Phys.* **31**, S352–S353 (1960).
- Pesquera, D. et al. Surface symmetry-breaking and strain effects on orbital occupancy in transition metal perovskite epitaxial films. *Nat. Commun.* **3**, 1189 (2012).
- Nakajima, R., Stohr, J. & Idzerda, Y. U. Electron-yield saturation effects in L-edge x-ray magnetic circular dichroism spectra of Fe, Co, and Ni. *Phys. Rev. B* **59**, 6421–6429 (1999).
- Schwicker, M. M., Guo, G. Y., Tomaz, M. A., O'Brien, W. L. & Harp, G. R. X-ray magnetic linear dichroism in absorption at the L edge of metallic Co, Fe, Cr, and V. *Phys. Rev. B* **58**, R4289–R4292 (1998).
- Thole, B. T., Carra, P., Sette, F. & Vanderlaan, G. X-Ray circular-dichroism as a probe of orbital magnetization. *Phys. Rev. Lett.* **68**, 1943–1946 (1992).
- Carra, P., Thole, B. T., Altarelli, M. & Wang, X. X-ray circular dichroism and local magnetic fields. *Phys. Rev. Lett.* **70**, 694–697 (1993).
- Wu, T. et al. Domain engineered switchable strain states in ferroelectric (011) [Pb(Mg_{1/3}Nb_{2/3})O₃]_(1-x)[PbTiO₃]_x (PMN-PT, x≈0.32) single crystals. *J. Appl. Phys.* **109**, 124101 (2011).
- Hu, J. M., Li, Z., Chen, L. Q. & Nan, C. W. High-density magnetoresistive random access memory operating at ultralow voltage at room temperature. *Nat. Commun.* **2**, 553 (2011).
- Wu, T. et al. Giant electric-field-induced reversible and permanent magnetization reorientation on magnetoelectric Ni(011) [Pb(Mg_{1/3}Nb_{2/3})O₃]_(1-x)[PbTiO₃]_x heterostructure. *Appl. Phys. Lett.* **98**, 012504 (2011).



This work is licensed under a Creative Commons Attribution 4.0 International License. The images or other third party material in this article are included in the article's Creative Commons license, unless indicated otherwise in the credit line; if the material is not included under the Creative Commons license, users will need to obtain permission from the license holder to reproduce the material. To view a copy of this license, visit <http://creativecommons.org/licenses/by/4.0/>

© The Author(s) 2017

Supplementary Information accompanies the paper on the *npj Quantum Materials* website (doi:10.1038/s41535-017-0020-0).